

SciEn Conference Series: Engineering Vol. 3, 2025, pp 637-642

https://doi.org/10.38032/scse.2025.3.160

Influence of Surface Temperature on The Hydrodynamic Characteristics for Flow over Rotational Cylinder

Sayedul Islam*, Abdullah Al-Faruk

Department of Mechanical Engineering, Khulna University of Engineering & Technology, Khulna-9203, Bangladesh

ABSTRACT

Turbulent flow over a rotational cylinder produces lift due to pressure differences on the upper and lower surfaces. The present numerical analysis focuses on the effect of the rotating cylinder's surface temperature. Simulations are carried out at the Reynolds number of 5000 for a series of velocity ratios ($\alpha = 0$ to $\alpha = 5$). The surface temperature varied from 300 K to 500 K. A temperature-variable viscous model is used for the simulations as fluid viscosity depends on temperature. Results from the simulation show that the increased surface temperature of the cylinder for the velocity ratio below 3 slightly improves the lift coefficient. However, for higher velocity ratios (4 to 5), a significant improvement in the lift coefficient is found. In the case of the drag coefficient, however, values increase infinitesimally. The flow streamlines are around the cylinder, and the stagnation point is attached to the cylinder surface for $\alpha \le 3$. On the other hand, the streamlines fold around the cylinder, creating an Envelope Vortex at $4 \ge \alpha \le 5$.

Keywords: Velocity Ratio, Reynolds Number, Lift Coefficient, Drag Coefficient, Vortex.



Copyright @ All authors

This work is licensed under a Creative Commons Attribution 4.0 International License.

1. Introduction

A rotating cylinder in Newtonian fluid that generates lift due to asymmetric flow is known as the Magnus force [1]. According to Bernoulli's principle, rotation creates a pressure difference between two-cylinder sides that creates lift. As the viscous force on the cylinder surface causes the fluid particles to rotate with the cylinder, it accelerates flow on one side and decelerates flow on the other. Flow over a cylinder has been of common interest in fluid machines. The fluid's viscosity is temperature-dependent. If the temperature changes, fluid viscosity will change, which may considerably affect the lift and drag coefficient.

Many researchers have studied the behavior of incompressible flow around rotating cylinders using computational and experimental techniques. Prandtl, one of the leading researchers in this discipline, examined rotating cylinders with different length-to-diameter ratios and determined that the lift coefficient had an upper limit of 4π [2]. Nonetheless, Tokumaru and Dimotakis were able to surpass Prandtl's recommended top limit in terms of lift coefficients [3]. Glauer experimental results show that at higher values of α , flow separation is reduced, and circulation rises with α but has no upper limit [4].

One of the main characteristics of flow over a rotating cylinder is that it creates the shedding of vortices. Shedding of vortices is also defended on the value of α . For $\alpha < 2$, Karman vortex is present. In the case of $4.4 \le \alpha \ge 4.8$ Shedding of vortices occurred on one side. In other values of α on shedding occurs [5-8].

Canuto and Taira's numerical analysis showed that at *Re* from 20 to 100 and Mach number from 0 to 0.5, the growth rate and frequency of linear instability for cases above the critical Reynolds number are identified, revealing that the frequency of the Kármán vortex street increases with Reynolds number [9].

At a larger Reynolds number turbulent flow past a rotating cylinder shows that the load coefficient shows an inverse relationship with the Reynolds number across all the values of spin rates. Turbulent kinetic energy and shear stress intensify nonlinearly with spin rates, peaking near the stagnation point [10].

Nagata et al. numerical analysis on the surface temperature effect in subsonic and supersonic flow shows that vortex shedding can be seen when the temperature ratio is less than unity drag coefficient increases with temperature ratio [11]. Salimipour and Anbarsooz investigate the effect of the rotating cylinder's surface temperature at Re = 200, M_{∞} from 0.1-0.4. Increasing the cylinder surface temperature reduces the lift coefficient, whereas the drag coefficient shows no pattern. For those Mach numbers, the study shows that the lift coefficient is reducing with a rising temperature ratio [12]. Paramane and Sharma investigate forced convection heat transfer across a rotating circular cylinder, focusing on a range of Reynolds numbers (20-160) and velocity ratios (0-6) to understand flow transitions and heat transfer characteristics and found how rotation can suppress vortex shedding and reduce heat transfer rates by creating thermal resistance through an enveloping vortex [13].

The previous studies have primarily examined the effects of cylinder surface temperature in an air medium, the current research shifts focus to a water medium, which introduces new complexities due to the temperature dependence of water's viscosity. By employing a viscous model tailored for water, this study investigates the resulting variations in lift and drag coefficients, providing novel insights into fluid dynamics in thermally sensitive aquatic environments.

2. Numerical model development

The governing equations for the present work are the continuity equation, 2-D Navier-Stokes, and energy equation, which are given below, respectively [14]

$$\nabla \cdot v = 0 \tag{1}$$

$$\rho(v \cdot \nabla)v = -\nabla p + \mu \nabla^2 v \tag{2}$$

$$\rho c_n(v \cdot \nabla T) = k \nabla^2 T \tag{3}$$

Where, v is the velocity, p is the pressure, μ is the viscosity, ρ is the density, c_p is the specific heat at constant pressure, and k is the thermal conductivity.

Polynomial equations were used to obtain temperaturedependent viscosity from Eq.(4). The polynomial coefficient values are given in the literature [15].

$$\mu = A_0 + A_1 T + A_2 T^2 + A_3 T^3 + A_4 T^4 + A_5 T^5 \tag{4}$$

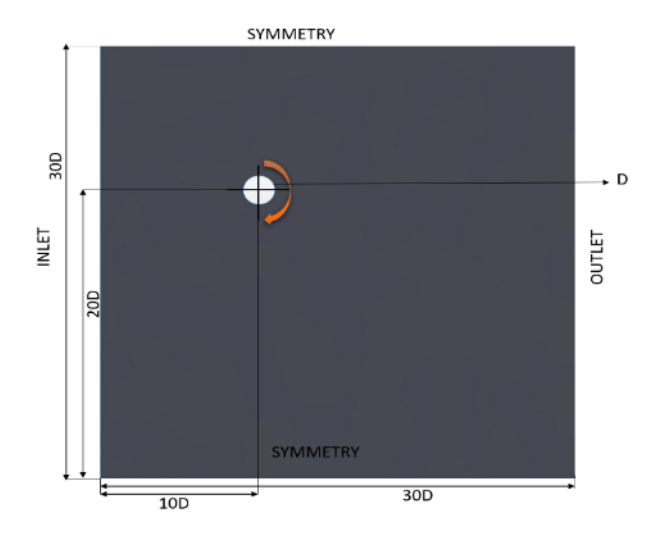


Fig.1 Computational domain consisting of the rotational cylinder.

Fig.1 shows a cylinder with diameter D and surface temperature T_s submerged in water with uniform fluid flow rotating with angle velocity ω in the clockwise direction. The inlet gauge pressure is zero. For the diameter D, the flow field Re = 5000. Where Eq.(5) gives the Reynolds number.

$$Re = \frac{\rho U_{\infty} D}{\mu} \tag{5}$$

Where U_{∞} is the free steam velocity, ρ is the density of water, and μ is the viscosity of water at freestream temperature. For dimensional analysis, the cylinder tangential velocity and free stream velocity ratio are known as the velocity ratio α , as shown in Eq.(6).

$$\alpha = \frac{\omega D}{2U_{\infty}} \tag{6}$$

The forces acting on the cylinder surface are lift and drag coefficients.

$$C_d = \frac{D}{\frac{1}{2}\rho U_{\infty}^2 D} \tag{7}$$

$$C_l = \frac{L}{\frac{1}{2}\rho U_\infty^2 D} \tag{8}$$

Where D is the drag force and L is the lift force. Another critical parameter for the observation is the pressure coefficient C_p .

$$C_p = \frac{p - p_{\infty}}{\frac{1}{2}\rho U^2_{\infty}} \tag{9}$$

Where, p_{∞} denotes the free stream pressure and p is cylinder surface pressure.

The simulation is performed in ANSYS 2020 R1 by considering a conservative second-order upwind is used. For the values of $\alpha \le 3$ SST k- ω model is used as this model gives accurate values at the surface wall and for $3 < \alpha \le 5$ Spalart-Allmaras model is used as its 1-D equation gives a more accurate value when the flow is separated. Here, pressure and velocity are coupled.

Fig.2 shows the mesh of the present computational domain. Mesh independence must be tested to obtain correct visualization. In this study, a structural mesh is used to minimize computational time. Mesh is biased in the surface region of the cylinder as the viscous sublayer is a crucial factor. y^+ <1 is considered in the cylinder surface.

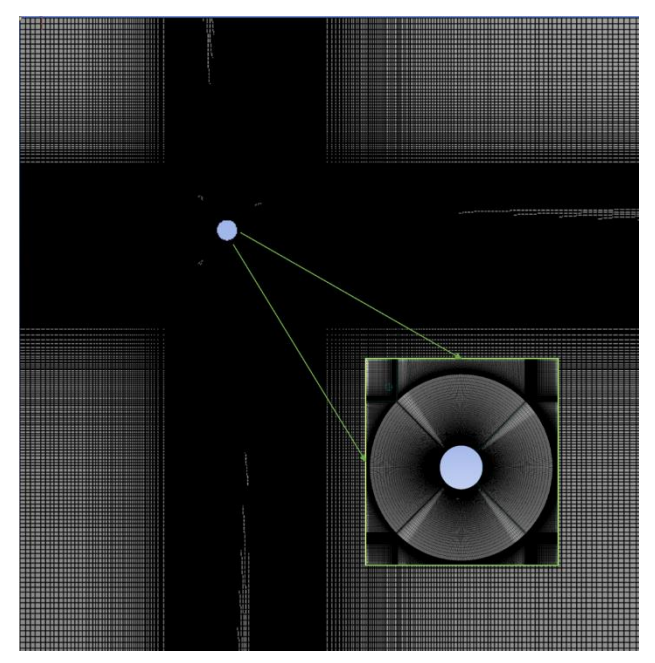


Fig.2 Mesh of the computational domain.

In Fig.3, the value of C_d becomes constant after 200000 elements. For the present study, around 500000 elements are chosen.

The results of the present study are compared with Aljure et al. to validate the numerical procedure [16]. Fig. 4 shows the lift coefficient values of both studies. Each study shows that results are the same at a lower value of α , but the present study gives higher values of lift coefficient for $\alpha > 3$.

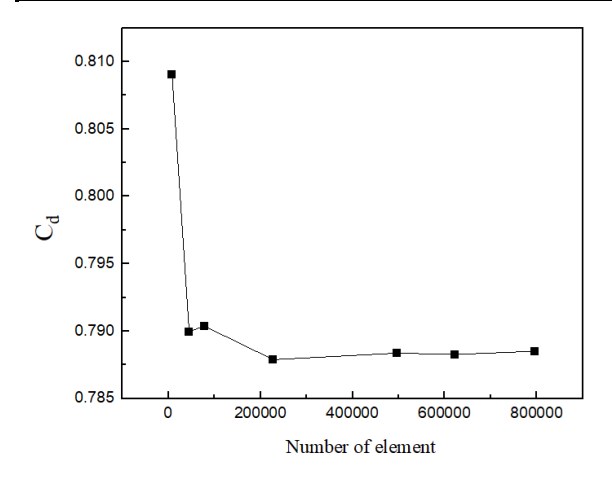


Fig.3 Variation of C_d along the number of elements.

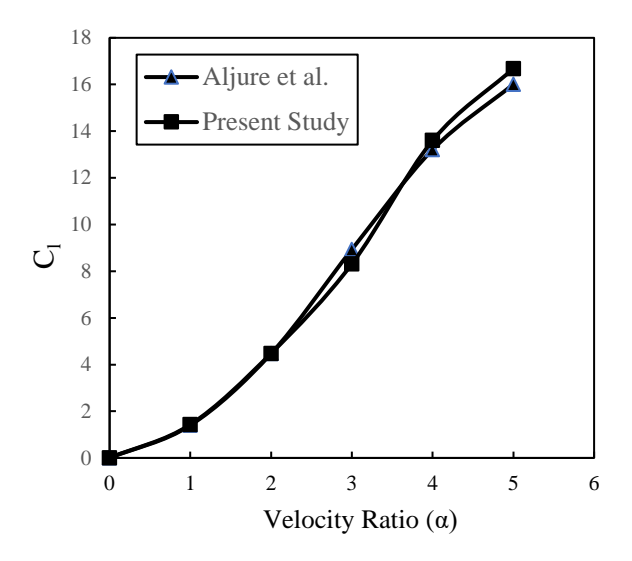
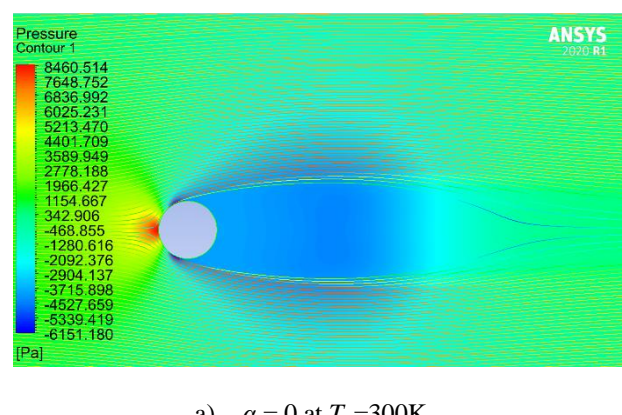


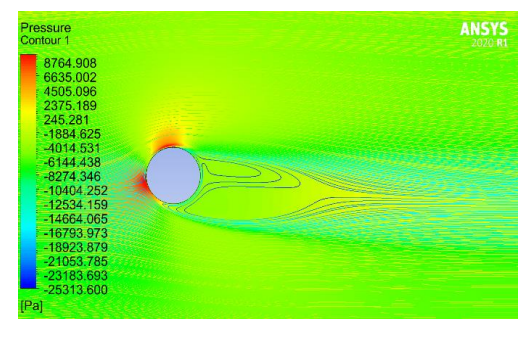
Fig.4 Comparison of lift coefficient between the present study and Aljure et al.[16].

3. Results and Discussion

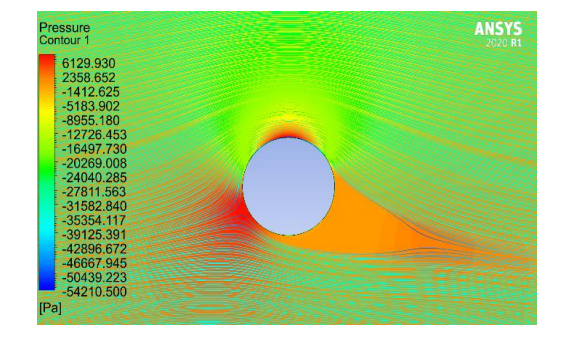
Fig.5 shows the flow around the cylinder at different velocity ratios. The figure shows pressure streamline couture at the cylinder surface temperature of 300 K.



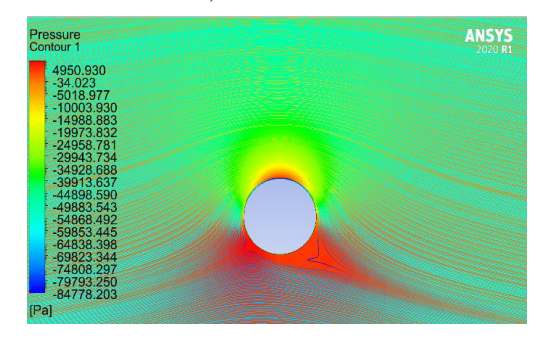
 $\alpha = 0$ at $T_s = 300$ K



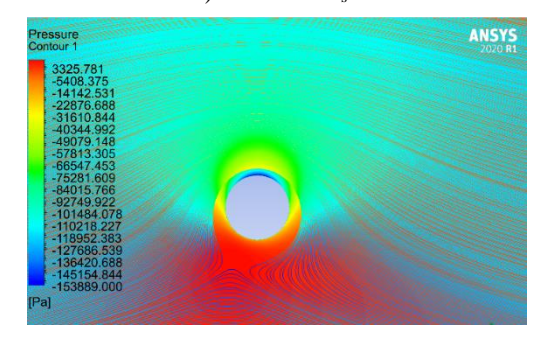
 $\alpha = 1$ at $T_s = 300$ K



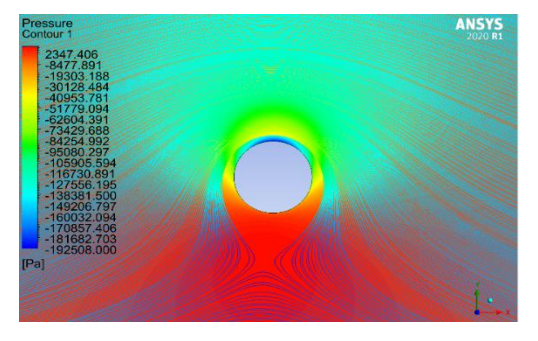
b) $\alpha = 2$ at $T_s = 300$ K



c) $\alpha = 3$ at $T_s = 300$ K



d) $\alpha = 4$ at $T_s = 300$ K



e) $\alpha = 5$ at $T_s = 300$ K

Fig.5 Pressure and Streamline Contour for the variation of velocity ratio from 0 to 5 at $T_s = 300 \text{ K}$

From the Fig.5 for $\alpha=0$, fluid flows over the cylinder, creating a stagnation point on the cylinder surface. Fig.5 shows that the pressure distribution around the upper and lower surfaces is almost the same, so no lift is generated. The cylinder creates a barrier to the flow and produces drag, and the stagnation point is on the cylinder surface.

When the cylinder starts to rotate, fluid velocity on the upper surface is more than on the lower surface. As a result of the Bernoulli effect, pressure on the upper surface is reduced, which generates lift. For $\alpha=1$, the stagnation point position is changed, and streamlines show that vortex size is reduced in the upper section along the horizontal axis. Again, $\alpha=3$ vortex size is reduced and slightly visible at the lower section of the cylinder. The stagnation point moves from the free stream velocity.

In the case of $\alpha=4$ and $\alpha=5$, the streamlines fold outside the cylinder creating an Envelope Vortex. The stagnation point is located outside the cylinder, but for $\alpha=0$ to $\alpha=3$, it is on the cylinder surface.

To analyze the effect of the cylinder surface temperature, the cylinder surface temperature varied from 300 K to 500 K. The coefficient of lift value for those observations is shown in Fig.6. Fig.6 shows that at a lower value of $\alpha \leq 3$, the lift coefficient mostly stays the same. Because at a lower velocity ratio, the surrounding fluid temperature increases slightly, which causes a slight change in the fluid's viscosity, a small improvement in lift coefficient is noticed. At 500 K cylinder surface temperature for $\alpha = 4$ and $\alpha = 5$, the lift coefficient improves around 11.21% and 24.04% compared to 300 K. This is because a higher surface temperature value creates a thermal boundary layer, as shown in Fig.7. Heat transfer from the cylinder to the water will decrease the viscosity of the water near the surface since viscosity decreases with increasing temperature in liquids. Lower viscosity near the cylinder due to heating will alter the boundary layer's dynamics, leading to a thinner boundary layer formation and improved circulation that generates a higher value of lift coefficient. From Fig. 8, pressure is reduced at the upper halves at 500 K temperature when velocity ratio 5 compared to 300 K, as shown in Fig.5 (f).

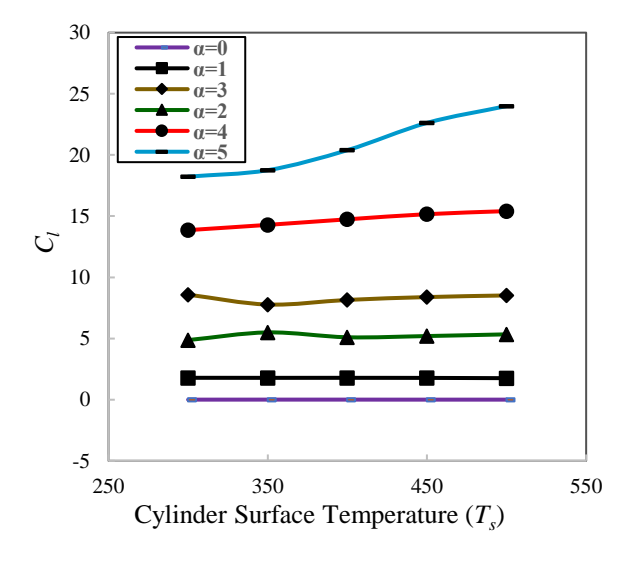


Fig.6 Variations of lift coefficient at different cylinder surface temperatures.

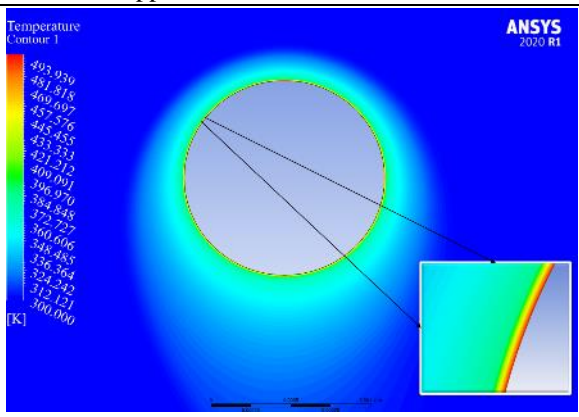


Fig.7 Cylinder Surface Temperature at 500 K at $\alpha = 5$.

The drag coefficient does not follow any trend with cylinder surface temperature. Fig.9 shows the effect of the cylinder surface on the drag coefficient. It is observed that $\alpha = 0$ to $\alpha = 4$ does not change very much and becomes almost the same for all cylinder surface temperatures, but for $\alpha = 5$, it shows that from 350 K temperature, the drag coefficient starts to increase and rise to the highest value of the drag coefficient in the numerical analysis. The reason for this behavior is unknown.

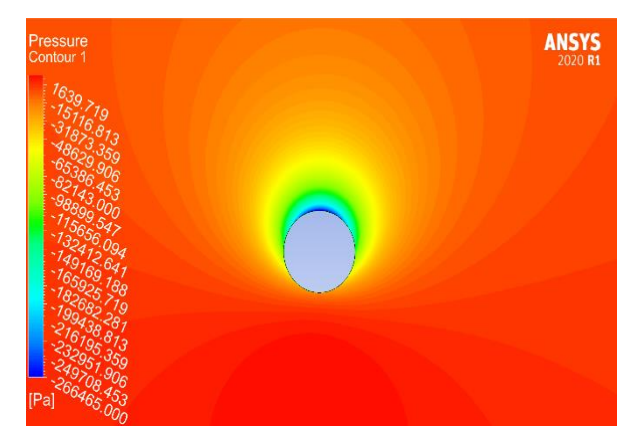


Fig.8 Pressure contour at 500 K and $\alpha = 5$

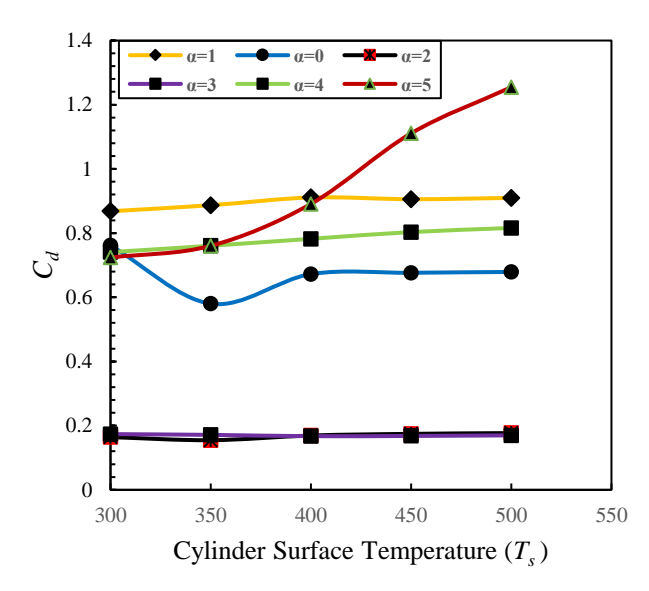


Fig.9 Variations of drag coefficient at different cylinder surface temperatures.

Table 1 C_l/C_d ratio for velocity ratio and surface temperature						
α	0	1	2	3	4	5
300K	0	2.05	29.66	49.42	18.7	25.18
350K	0	2	35.51	45.4	18.78	24.67
400K	0	1.95	30.12	48.76	18.84	22.89
450K	0	1.96	29.8	49.93	18.87	20.36
500K	0	1.93	30.18	50.19	18.88	19.12

Table 1 gives the ratio of lift and drag coefficient. From the given data, it is observed that for $0 \le \alpha \le 3$ the lift and drag ratio rises for increasing the surface temperature values after $\alpha = 4$ lift and drag ratio value is reduced. At $\alpha = 0$, the lift and drag ratio is always zero. For $\alpha = 1$ and $\alpha = 5$, increasing the surface temperature decreases the lift and drag ratio. At $\alpha = 4$, the lift and drag ratio is almost constant for all surface temperatures.

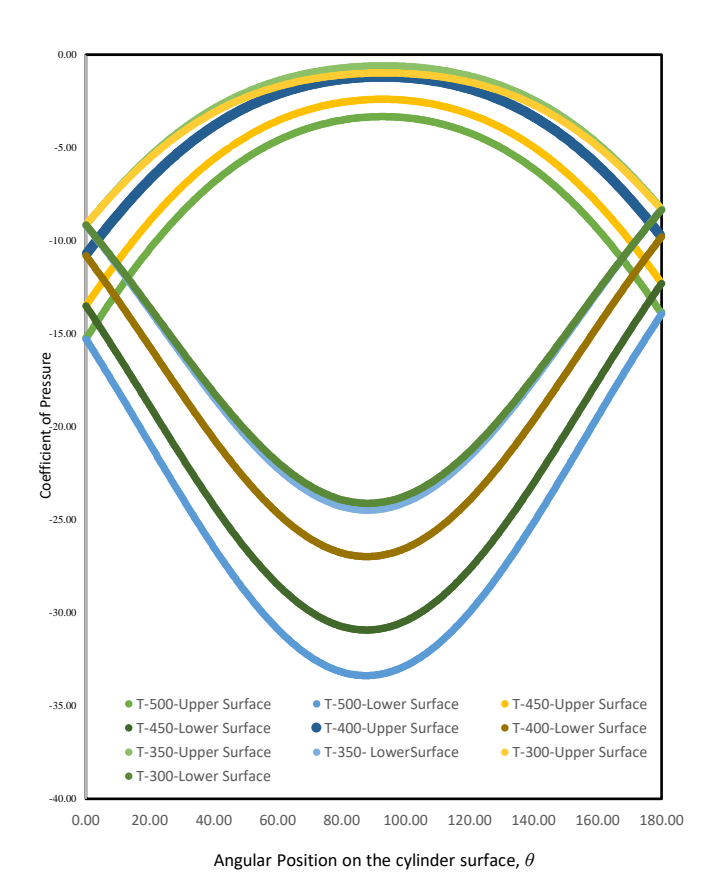


Fig.10 Variation of pressure coefficient (C_p) at different cylinder surface temperatures (T_s) for velocity ratio $\alpha = 5$.

The pressure coefficient plays a pivotal role in generating the lift coefficient. Fig.10 shows the changes in the pressure coefficient with surface temperature; the upper halves of the curve represent the cylinder's upper surface, and the lower halves represent the lower surface. Fig.10 shows that increasing surface temperature in the case of $\alpha=5$ causes a decrease in the pressure coefficient in the upper halves, but rising surface temperature increases the pressure coefficient for the lower surface. This difference in pressure coefficient due to surface temperature causes an increasing lift coefficient in a higher velocity ratio.

4. Conclusion

This numerical analysis presents the effect of the cylinder surface temperature on fluid flowing in a rotating cylinder at different velocity ratios. The rotation of the cylinder creates vortexes that tend to change with the velocity ratio. At a velocity ratio of $0 \le \alpha \le 3$, vortexes are around the cylinder. For the velocity ratio $4 \le \alpha \le 5$ an envelope vortex is generated, creating a stagnation point outside the cylinder. The numerical approach indicates that the lift coefficient of the rotating cylinder when $\alpha = 4$ the surface temperature is 500K and increases by 11.21% compared to 300 K. The lift coefficient is further improved by 24.04% for $\alpha = 5$ compared with the surface temperature at 300K and 500 K. The drag coefficient increased by 84.81% compared to α =0 with α = 5 at 500 K surface temperature. For all $0 \le \alpha \le 4$ the lift and drag ratio gives almost similar values, but at α =5, the lift and drag ratio reduces from 25.18 to 19.12 for the surface temperatures 300 K and 500 K. At velocity ratio 5, when the surface temperature is 500 K, shows a significant rise in the coefficient of pressure at the lower halves of the cylinder compared to other temperatures.

References

- Seifert, J., A review of the Magnus effect in aeronautics, Progress in Aerospace Sciences, vol. 55, pp. 17-45, 2012.
- [2] Prandtl, L., Application of the "Magnus effect" to the wind propulsion of ships, 1926.
- [3] Tokumaru, P., Dimotakis, P., Rotary oscillation control of a cylinder wake, Journal of Fluid Mechanics, vol. 224, pp. 77-90, 1991.
- [4] Glauert, M., The flow past a rapidly rotating circular cylinder, Proceedings of the Royal Society of London. Series A. Mathematical and Physical Sciences, vol. 242, no. 1228, pp. 108-115, 1957.
- [5] Rao, A., Radi, A., Leontini, J. S., Thompson, M. C., Sheridan, J., Hourigan, K., A review of rotating cylinder wake transitions, Journal of Fluids and Structures, vol. 53, pp. 2-14, 2015.
- [6] Kumar, S., Cantu, C., Gonzalez, B., Flow past a rotating cylinder at low and high rotation rates, Journal of Fluids Engineering, vol. 133, no. 4, p. 041201, 2011.
- [7] Mittal, S., Kumar, B., Flow past a rotating cylinder, Journal of Fluid Mechanics, vol. 476, pp. 303-334, 2003.
- [8] Coutanceau, M., Menard, C., Influence of rotation on the near-wake development behind an impulsively started circular cylinder, Journal of Fluid Mechanics, vol. 158, pp. 399-446, 1985.
- [9] Canuto, D., Taira, K., Two-dimensional compressible viscous flow around a circular cylinder, Journal of Fluid Mechanics, vol. 785, pp. 349-371, 2015.
- [10] Karabelas, S., Koumroglou, B., Argyropoulos, C., Markatos, N., High Reynolds number turbulent flow past a rotating cylinder, Applied Mathematical Modelling, vol. 36, no. 1, pp. 379-398, 2012.
- [11] Nagata, T., Nonomura, T., Takahashi, S., Mizuno, Y., Fukuda, K., Direct numerical simulation of flow around a heated/cooled isolated sphere up to a Reynolds number of 300 under subsonic to supersonic conditions, International Journal of Heat and Mass Transfer, vol. 120, pp. 284-299, 2018.

- [12] Salimipour, E., Anbarsooz, M., Surface temperature effects on the compressible flow past a rotating cylinder, Physics of Fluids, vol. 31, no. 2, 2019.
- [13] Paramane, S. B., Sharma, A., Numerical investigation of heat and fluid flow across a rotating circular cylinder maintained at constant temperature in 2-D laminar flow regime, International Journal of Heat and Mass Transfer, vol. 52, no. 13-14, pp. 3205-3216, 2009.
- [14] Blazek, J., Computational fluid dynamics: principles and applications, Butterworth-Heinemann, 2015.
- [15] Wang, C., Liu, S., Wu, J., Li, Z., Effects of temperature-dependent viscosity on fluid flow and heat transfer in a helical rectangular duct with a finite pitch, Brazilian Journal of Chemical Engineering, vol. 31, pp. 787-797, 2014.
- [16] Aljure, D., Rodríguez, I., Lehmkuhl, O., Pérez-Segarra, C. D., Oliva, A., Influence of rotation on the flow over

a cylinder at Re= 5000, International Journal of Heat and Fluid Flow, vol. 55, pp. 76-90.

NOMENCLATURE

 U_{∞} : Freestream velocity, m·s⁻¹

 $D\;$: Diameter of the cylinder, m

 ω : Angular velocity, rad·s⁻¹

 α : Velocity ratio

Re: Reynolds number

p: Cylinder surface pressure, Pa

 C_d : Drag Coefficient

 C_l : Lift Coefficient

 ρ : Density, kg·m⁻³

 μ : Viscosity, Pa·s

 T_s : Surface temperature, K

D: Drag force, N

L: Lift force, N